

Enhancing Diabetic Retinopathy Detection and Grading through Contract-Expansive U-Net Model for Accurate Severity Prediction and Timely Intervention

Sweta¹, Dr. Ritu Sindhu²

¹PhD. Scholar, Lingaya's Vidyapeeth, rishu.sweta@gmail.com

²Professor, Lingayas Vidyapeeth, ritu.sindhu2628@gmail.com

Diabetic retinopathy (DR) is a leading cause of vision impairment and, if left untreated, can lead to irreversible damage to eyesight. As the disease progresses, the potential for vision recovery diminishes, making early and accurate detection crucial for effective intervention. Currently, the existing detection methods have a problem of lack of precision in terms of the severity of the disease and are vulnerable to misleading in such severe cases, which has made it difficult for ophthalmologists to effectively manage the DR, and thus, there is an acute need to make improvements in the detection methods that are available to achieve time-bound precise care. Probably, the most crucial steps involved in the management of DR are the accurate predictions and grading of its severity. This does not allow clinicians to make predictions about the progression of the disease and choose an appropriate treatment strategy. All this increases the workload for medical professionals, which, of course, complicates management even more. These difficulties, therefore, may require a Contract-Expansive U-Net model that is geared toward the enhancement of DR detection and grading. The encoder-decoder design uses the autoencoder concept which allows it to capture the minor details of the retinal images and, thus, the encoder-decoder structure allows both the complex and simple computations of retinal images to be carried out. Through the use of sophisticated classification algorithms and optimization techniques, the model not only enables the early detection of DR symptoms but also ensures a more accurate diagnosis for the serious cases. This method is not only able to increase the detection accuracy, but also, because of the velocity of the intervention, the burden on the ophthalmologist is reduced which, in the end, is one of the prerequisites for the patient's better outcome, namely the proper treatment approach.

Keywords: Diabetic Retinopathy, Severity Grading, Contract-Expansive U-Net, Disease Detection, Optimization Techniques and Segmentation.

1. Introduction

Diabetes-related retinopathy (DR) is a very bad eye disease that can even lead to the loss of sight to people with diabetes. Adults and adolescents who have had diabetes for a long time are prone to this secondary factor of diabetes mellitus. As per research, the number of people

who are affected by DR and have a progressive form is 17 million, which is about 93 million worldwide. DR is one of the leading causes of blindness by now. Diabetic macular oedema affects 21 million people worldwide. The diabetic macular oedema comprises 21 million people worldwide. “A retinal disease that comes out as a complication of diabetes is the condition identified as diabetic retinopathy (DR). Diabetes in people for a long period is a risky contributor to the damage of blood vessels of the retina. Through investigations, high blood sugar levels, long period of diabetes, and high blood pressure are the straight deviants of the condition. With 18% of those afflicted, DR is highly prevalent in urban populations in India, with men being more vulnerable. High blood sugar levels harm the retina's blood vessels, causing leakage and oedema in diabetic retinopathy, also referred to as diabetic eye disease. In extreme situations, the retina's blood supply might be cut off. This might eventually cause serious harm to the retina, which is frequently the main reason why diabetes individuals become blind.

Regardless of whether one suffers from type 1 or type 2 diabetes, diabetic retinopathy can occur in any diabetic. Diabetes can be fatal, but it can also be managed, treated, and managed to enable people live normal lives but if unattended, diabetes can damage nerves, eyesight, and may even lead to infections, mostly in the feet.

The key reason why early diabetic retinopathy should be diagnosed is in saving quality of life as well as in stopping more further visual loss. It has become feasible to avoid blindness in the majority by the prevention through early diagnosis and treatment. Thus, in order to prevent people suffering at distant places due to scarcity of health infrastructures, scarce knowledge of physicians as well as improper means of investigations; it becomes imperative nowadays to evolve an automated diagnostic scheme for detecting diabetic retinopathy. This research proposal postulates a machine-learning grading procedure for diabetic retinal disease which can abolish the requirement of manual assessments; with the use of computer vision and artificial intelligence to process massive data-sets and furnish accurate responses within short durations. Diabetic retinopathy is a potentially dangerous eye condition that leads to blindness among diabetics. Both adults and adolescents are susceptible to this secondary consequence of diabetes mellitus. According to research, 93 million inhabitants of the world are suffering from DR. Among them, 17 million are suffering from the most severe form-proliferative DR. DR has become one of the main causes of blindness in the world. According to [2], diabetic macular oedema affects 21 million persons globally. Prolonged diabetes duration, high cholesterol levels, and inadequate blood sugar control are directly linked to the condition.

With 18% of those afflicted, DR is highly prevalent in urban populations in India, with men being more vulnerable. High blood sugar levels harm the retina's blood vessels, causing leakage and oedema in diabetic retinopathy, also referred to as diabetic eye disease. In extreme situations, the retina's blood supply might be cut off. This might eventually cause serious harm to the retina, which is frequently the main reason why diabetes individuals become blind.

Regardless of whether one suffers from type 1 or type 2 diabetes, diabetic retinopathy can occur in any diabetic. Diabetes can be fatal, but it can also be managed, treated, and managed to enable people live normal lives. But if left unchecked, diabetes can harm nerves, eyesight, and even lead to infections, especially in the feet.

Diagnosing diabetic retinopathy early is essential to preserving quality of life and halting

additional visual loss. With early diagnosis and therapy, blindness can be prevented for many people. Thus, it is now more crucial than ever to develop an automated approach to identify diabetic retinopathy, particularly in places with inadequate healthcare infrastructure and knowledge. Using computer vision and neural networks to evaluate massive datasets and provide precise answers rapidly, this work suggests an automated grading tool for diabetic eye disease that can eliminate the need for physical evaluations. The major contribution of the proposed model is,

- The proposed Contract-Expansive U-Net model improves the detection accuracy of diabetic retinopathy by using its encoder-decoder architecture to extract and reconstruct fine-grained details from retinal images, thus allowing for the accurate identification of DR stages and severity grading.
- Advanced classification and optimization techniques would integrate multiple classifiers, allowing optimization methods to be incorporated in the process. Such a method would make possible accurate assessment of the course of DR, improving prognosis and intervention planning according to patient status.
- This model will improve the detection of DR. This reduces the workload of the medical practitioner to a considerable extent, ensuring a timely and well-informed treatment decision in order to further improve patient care and outcome.

2. Literature review

For people with diabetes for a long time, diabetic retinopathy is a leading cause of blindness and vision impairment. Since it can help ophthalmologists manage the increasing number of patients and data records with less manual labour, accurate detection of this condition is a major area of focus for researchers.

2.1. Investigation on image processing-based detection

When using machine learning-based techniques to diagnose diabetic retinopathy, preoperative photos are crucial for spotting critical characteristics including exudates, microaneurysms, and scarlet fever. To increase detection accuracy, a variety of techniques have been employed in the past. (2014) concentrated on morphological techniques for fundus imaging exudate detection. Similar methods were employed by [3] to identify leaks in the Messidor and Drive datasets using intensity, power-up transformation, and comparative enhancement. In order to identify red images and categorise them into severity, amount, and normality, they also employed histogram matching and blood flow detection. While the first method used the intensity and origin by recognising vessels, the second process used edge detection and morphological processes. Also used dynamic thresholding, picture removal, median filtering, and image aggregation to identify complicated leaks. [4] improved the detection of microaneurysms and exudates by utilising image scaling, contrast enhanced histogram equivalent (CLAHE), and peak filters. Additionally, vascular ablation is employed to enhance microaneurysm identification. Combining many scanning techniques and candidate extraction tactics to score retinal microaneurysms. They employed CLAHE and the cyclic Hough transform for processing and final results after employing picture enhancement and extraction

techniques. Because exudates are close to the foveal region, [5] employed image processing techniques such brightness contrast, green channel extraction, and optic disc and macula expression to determine the amount of exudates in hard tissue.

In order to enhance contrast and detection capabilities, changed the fundus image from the DiaretDb database to green channel in order to detect yellow lesions. They employ CLAHE to improve illumination, morphological approaches to eliminate background, and an expanding area algorithm to identify exudates. Similar methods for identifying challenging exudates, enhancing light quality, performing open surgery, fractures, and optic disc ablation, as well as using a median filter to enhance picture quality, were proposed by [6]. In order to stop the virus from spreading, they also employed detection techniques like the Kirsch algorithm to find exudates. identified diabetic retinopathy by looking for exudates and microaneurysms in a small dataset of 30 retinal pictures. They set up the optical equipment, apply the contrast approach, and convert the colour image to IHS format while concentrating on the area that has changed the most. Employ an iterative region development technique to identify leaks and a neural network to extract blood vessels. Additionally, the red virus and the orange backdrop were separated using the operator trench efficient automatic categorisation and control systems.

2.2. Investigation on machine learning based detection

The related work involves detection and classification of microaneurysms and exudates in fundus images. They applied morphological operations to eliminate blood vessels, while the feature extraction techniques involved converting RGB images to CMY representation. Exudates and micro aneurysms were then obtained by applying hole-filling techniques, edge detection, and thresholding processes. All these were fed into decision tree and SVM classifiers for detection and classification.

A methodology for classifying the presence of exudates in retinal images was developed by [8]. In their approach, they applied several morphological operations to extract the optic disc, remove blood vessels, and detect exudates by using opening operations. With this information, they had developed and tested a Convolutional Neural Network that improved the accuracy for the detection of exudates.

A characterization technique based on AM-FM for analyzing fundus images was proposed by [9]. Authors used demodulation techniques combined with Gabor filters to detect edges and further textural as well as blood vessel information, which further classified diabetic retinopathy based on rules applied on those features using a Random Forest classifier.

[10] applied numerous preprocessing techniques, including the use of thresholding to enhance the image, making it binarized then removing blood vessels. As mentioned earlier, the focal point was on micro aneurysms. Further, they used Gaussian Mixture Models to identify their existence and classify the severity based upon the number of red lesions.

According to [11], diabetic retinopathy was divided into three grades: normal, dot haemorrhages, and exudates. Image addition and subtraction with the use of morphological operations were conducted by them for characteristic extraction in relation to optic disc and blood arteries. A feedforward neural network was utilized in this process for its training by classifying its features extracted.

[12] has used a soft margin SVM classification method for diabetic retinopathy based on exudates. They segmented the exudates with a set of morphological techniques such as image addition subtraction, and intensity thresholding. Then they used the segmented exudates to extract area, perimeter, and standard deviation, which were further passed to the SVM classifier. A CNN algorithm was also used by [13] to detect exudate in fundus photos. Over the lighted fundus images and green channel pixels, they applied a 64x64 patch. Refinement of exudate extraction was aided by opening surgeries and the removal of optic discs. 82 photos from the e-optha database were used to test their approach.

CNNs were used by [14] to identify exudates and categorise whether diabetic retinopathy was present or not. Prior to entering the fundus photos into the model for training and testing, they pre-processed them by standardising their size and turning them into greyscale.

In order to identify exudates and haemorrhages, [15] used machine learning techniques in conjunction with picture preprocessing. They eliminated the optic disc and background information because they were thought to be memory-intensive but unrelated to the identification of diabetic retinopathy. Principal component analysis was used to visualise the features, which included mean and standard deviation, that were taken out of each image channel. After that, SVM was used for classification

A technique for identifying exudates, micro aneurysms, and haemorrhages was presented by [16]. They divided fundus photos into groups such as those with proliferative, non-proliferative, and no diabetic retinopathy. They integrated textural information into an artificial neural network and SVM for classification, using Gaussian filters to remove blood vessels and automatic mask construction on pictures from DRIVE and DIARETDB databases.

[17] classified diabetic retinopathy into binary categories using machine learning models such as Naive Bayes, SVM, k-nearest neighbours (KNN), and decision trees. These models have been trained on the available photographs in the Messidor database. Other models performed pretty well but not as good as the SVM model because of lack of feature extraction and preprocessing.

These researches depict various machine learning and image preprocessing techniques that are exploited for diabetic retinopathy identification, such as classifier training, feature extraction, and morphological procedures. Preprocessing procedures such as removal of blood vessels and exudate segmentation improve the accuracy and performance of automated diabetic retinopathy classification systems.

Most of the recent efforts focus on characterizing features of diabetic retinopathy, or grading with the image processing techniques. In the current work, we had proposed a classification method with three severity levels-mild, moderate, and the severe diabetic retinopathies-for classifying and quantifying the exudates and microaneurysms of 1361 fundus images. This article presents a technique to predict the exudates and micro-aneurysms using methods of image processing, feature extraction, and models applied in machine learning that helps correctly predict the presence of such exudates and micro-aneurysms in the diabetic retinopathy images.. Table 1 provides a summary of the methods comparison covered in the literature review.

An O-shaped neural network with attention modules was proposed by [18] for junction

identification in biomedical pictures. It has high F-1 scores but is computationally costly. A fully attention-based network (FANet), which integrates multi-set data and learns features adaptively, was presented by [19]. However, it requires GPUs for computing and is time-consuming and sophisticated. [20] described a technique that uses wavelet responses to distinguish between thick and thin vessels in retinal pictures. Although accurate, this method's identification process is sluggish and it has trouble with pathological photos because of noise. CNNs were employed by [20] to detect exudates, but their model is computationally demanding and requires an extensive training dataset, making it unsuitable for smaller medical picture datasets. Comparing to deep learning models, our suggested method is more effective and uses less photos and computer power. The approach uses conventional lightweight machine learning algorithms for identification in conjunction with manually created image features that have been retrieved using image processing techniques. The grading procedure is divided into two parts: one counts the number of micro aneurysms, and the other concentrates on exudates according to their separation from the macula. In addition to being easier and less expensive, this approach yields accurate findings without the need for large datasets or potent GPUs.

Unlike the state-of-the-art deep learning-based methods, our methodology may be implemented with low CPU needs and is optimised to function effectively with smaller datasets.

3. Proposed Methodology

3.1. CONTRACT-EXPANSIVE U-NET MODEL FOR RETINAL DIABETIC PREDICTION

If DR is left untreated, it will lead to severe loss of vision. Vision recovery becomes more difficult with an advance of the illness. Thus, for the successful treatment of DR cases by ophthalmologists, it is vitally important that the currently available methods of DR detection be improved. For predicting accurately about DR's disease course, severity grading is indispensable. Several outputs of classifiers can be optimized through the use of an optimization technique to make an output decision that may accurately portray disease severity. From such integrated approaches, the early possibility of intervention and a full range of treatment become viable in addition to giving an overall evaluation of a patient's state of health. The vast potentials it offers to improve the patient outcomes and lighten the burden workload on the medical person would thus be seen in this aspect of introducing grading capabilities in the use of present DR detection technologies. Advanced classification algorithms and the procedures of optimization will guide the ophthalmologists in arriving at the correct decision with the treatment of the case of DR finally leading towards improvement in the patient's care and preserving vision.

3.2. DATA COLLECTION

A proper basis for DR analysis can be provided by DR datasets such as Messidor-2 [125] and IDRiD dataset [20]. To enhance the robustness and applicability of proposed methodologies, work is designed using various datasets. In addition to applied significance, Central Government Railway Hospital (ICF Hospital) real-time datasets ascertain a more

comprehensive investigation process of medical image processing methodologies. This collection of datasets shows a deliberate attempt in the inclusion of various sources, where the proposed approaches are examined and validated for further use in different clinical settings.

3.3. PROPOSED Contract-Expansive U-Net-GAN ARCHITECTURE

Figure 1 shows the IMDE-UGAN approach to classifying DR images. This approach uses real-time datasets for training, testing, and validation in addition to the Messidor and IDRiD collections as input images. The method of data segmentation and augmentation makes use of Net GAN. GAN segmentation and the ResNet encoder are used in image synthesis. The conditional GAN based on SPADE is used in the DR segmentation process. The segmented label precisely aligns the OD and vascular during the augmentation stage by using elastic stretching, turning, opening, and dilatation procedures. The discriminator classification network was modified to produce a decoder-encoder network, which is how the U-Net Generative Adversarial Network (U-Net GAN) was used for image classification. Using both global and local variations, the discriminator is in charge of differentiating between authentic and fraudulent photos. Through the judicious cutting and pasting of pieces from several image categories, the CutMix augmentation approach creates synthetic images. Lastly, the input DR photos are categorised into five grades according to the DR severity levels. Unbalanced data with least-represented classes is handled by CutMix augmentation. Datasets frequently have imbalanced classes; as a result of the random removal of unbalanced information, the training set has fewer data points from the majority class. Many original scanned photos are included in DR image analysis; however, undesirable images are later removed to guarantee useful results, prevent information loss, and prevent inappropriate issues. The purpose of data augmentation is to enhance visualisation. Following augmentation, the image's size was decreased from 256 x 256 pixels to 128 x 128 pixels. Here, CutMix augmentation is used. One popular method for regularising the model and expanding the dimension of the training datasets is data augmentation.

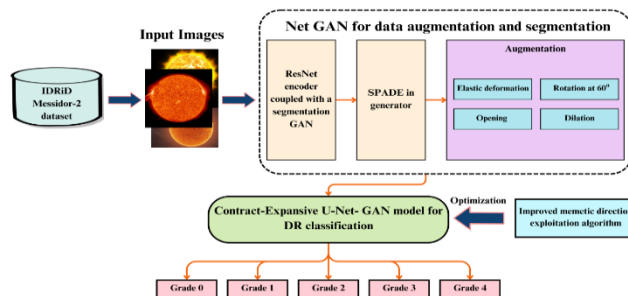


Figure 1. Propose Architecture of Severity Grading Model

3.3.1. Augmenting and Segmenting Images with Net GAN

The ResNet encoder-based GAN-based picture synthesis module is displayed in Figure 2. A segmentation-conditioned GAN is connected to the ResNet encoder. The generator model's SPADE normalization layers are used by GAN. To maintain the anatomy, SPADE-based GAN was utilized for vascular segmentation and DR to generate images of the OD. Realistic picture synthesis is made possible by using multi-class labels to guide the SPADE generator. The

generator's neighbor up sampling nearest layers come after SPADE normalization using residual blocks, and the resulting images encode input segmentation information. The ResNet encoder defines the appearance and anatomy of synthetic images by using retinal images to gather baseline vascular and OD information during synthesis. DR picture pairings with ground-truth segmentations made up the training dataset. Through label swapping and enhancement, the generator was trained to generate fresh pairs of simulated DR pictures. Rotation and morphological operations are applied to the segmented labels of the training set to produce the augmented labels. Unseen shapes can be produced and fed into the generator by rotating the scar and applying morphological processes. By mixing DR photos of healthy people with segmented labels from patients with problems, and vice versa, using swapped labels, new scenarios are produced. Rotation and elastic deformation techniques are used to improve lesion segmentation. Creating augmented and switched labels is part of acquiring data for blood stream segmentation. Because the blood artery is masked, changing the backdrop colour would not affect lesion segmentation; only the better labels are employed.

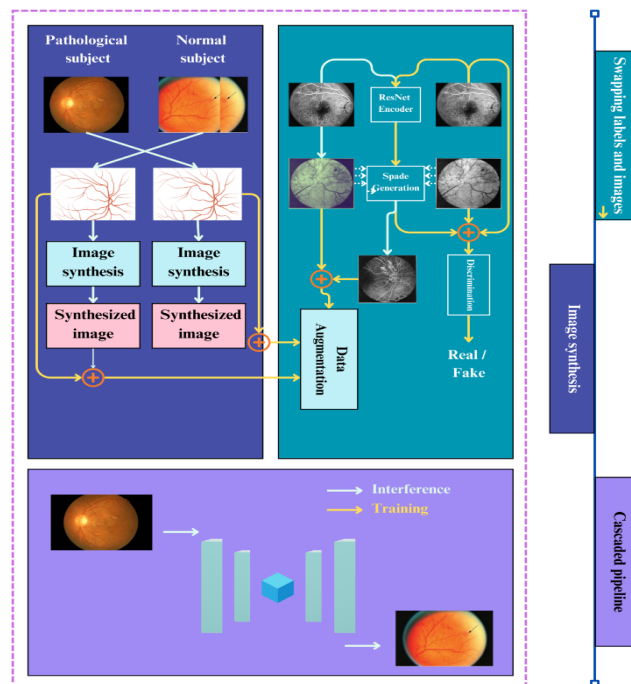


Figure 2. Image Synthesis based on GAN Model

3.3.2. LESION SEGMENTATION

The NV is located in the retina in any point within a 45-degree radius of the OD. NV are pouring into the brain from its most conspicuous location. Sometimes NV does not form any networks in the OD; instead, it grows on the retinal surface. The Region of Interest (ROI) and NV insertion site were identified using pathology statistical analysis. At or near OD, the likelihood of NV insertion is roughly 0.15; at another, it is 0.40; and at both, it is 0.45. A diagnostic test and particular techniques are used to calculate ROI. The local vascular characteristics inside the ROI region are precisely detected by this test. Additionally, it has

been determined that the ROI region should occupy 25% of the image.

3.3.3. VESSEL SEGMENTATION

To create a uniform initialisation procedure, the NV is placed into the pixels inside the vessels. Otsu thresholding is used on the image's green channel to identify pixels linked with vessels in order to perform a rudimentary vessel segmentation prior to implementing the bottom hat operator. The body of the segmented image is the name given to the final picture. The initial objective of the study was to employ U-Net to investigate intricate vascular segmentation. DR grading performance did not improve in spite of improvements in vascular segmentation. As a result, the best method is selected to grade the DR model.

3.3.4. SEGMENTATION OF OD

In addition to recognising and segmenting medical pictures, the OD was partitioned using the Net-GAN architecture. Several segmentation modules are used in the architecture to assess the items found in publically accessible datasets. The process of dividing a binary picture is referred to as D .

3.3.5. U-NET GAN CLASSIFIER

The encoder portion of the vanilla GAN is based on the U-Net design, and it consists of a Discriminator (D_r) and a Generator (G_r). It is able to differentiate between authentic and fraudulent photos and recognise various DR grading levels. The G_r wants to trick the D_r by creating realistic-looking graphics. By generating characteristics from the training data, using an encoder such as the D_r reduces overfitting. However, overfitting may result from U-Net's many parameters, such as skip connections and additional layers in the expanding route, particularly when working with small datasets. Lack of access to huge medical datasets, especially enormous photographs, is a major obstacle to using the U-Net discriminator model. The following goals must be methodically lowered in order to practice the GAN efficiently:

$$O_{D_r} = -F_a [\log D_r(a)] - F_c [\log (1 - D_r(G_r(c)))] \quad (1)$$

$$O_{G_r} = -F_c [\log D_r(G_r(c))] \quad (2)$$

Using formulas (6.1) and (6.2), r converts the variable into a realistic image appearance, and D_r separates the generated images from the genuine ones. The two types of convolutional networks are commonly represented by the symbols D_r and r . Although the architecture and objective properties of GAN may differ, improving the D_r network is essential. The architecture is changed to produce a U-Net-based D_r , maintaining local as well as global data representation, in order to enhance the DR network. This change guarantees the creation of a distinct GAN without changing the generator. Below is some information about the regularisation method and D_r based on U-Net.

3.3.6. Contract-Expansive procedure for DR grading

The input is down sampled by the encoder to capture the whole world optical environment, and then a decoder enlarges the image to match the initial input resolution in order to achieve precise localisation. D_r is modified in order to apply the U-Net concept. The D_r classifier block represents the encoder element, while the G_r networks block represents the decoder

component. Both further sampling and down sampling networks are used in this configuration in the Dr, represented by the symbol Dr . Using the actual discriminator Dr , the doctor determines if the incoming image is true (genuine) or false (fake). Furthermore, the U-Net Dr divides the image into either true or false regions by Dr according to the encoder's per-pixel classification. As a result, the doctor distinguishes between real and deceptive images on a local and global level.

Disparities between real and fake pictures, both local and worldwide. The constructed decoder block is called Dr^U_{decoder} and Dr^U_{encoder} , while Dr^U_{encoder} is the Dr's real encoder block. Equation (6.3) evaluates the recently developed Dr loss in this way.

$$O_{Dr^U} = O_{Dr^U_{\text{encoder}}} + O_{Dr^U_{\text{decoder}}} \quad (3)$$

The decoder loss $(O_{Dr^U_{\text{decoder}}})$ and an encoder loss $(O_{Dr^U_{\text{encoder}}})$ are evaluated using the following equations (4-6).

$$O_{Dr^U_{\text{encoder}}} = -F_a[\log Dr^U_{\text{encoder}}(a)] - F_c[\log (1 - Dr^U_{\text{encoder}}(Gr(c)))] \quad (4)$$

$$O_{Dr^U_{\text{decoder}}} = -F_a[\sum_{j,i} \log [Dr^U_{\text{decoder}}(a)]_{j,i}] - F_c[\sum_{j,i} \log (1 - [Dr^U_{\text{decoder}}(Gr(c))]_{j,i})] \quad (5)$$

$[Dr^U_{\text{decoder}}(a)]_{j,i}$ and $[Dr^U_{\text{decoder}}(Gr(c))]_{j,i}$ are Dr decisions in pixels (j, i) . Gr objectives can be turned into

$$O_{Gr} = -F_c[\log Dr^U_{\text{encoder}}(Gr(c)) + \sum_{j,i} [Dr^U_{\text{decoder}}(Gr(c))]_{j,i}] \quad (6)$$

3.3.7. Implementing U-Net-based Dr

In order to construct the U-Net, the input of each decoder ResNet module is linked to the corresponding encoder module's output characteristics, guaranteeing comparable resolutions. This makes the decoder structure similar to a Gr by combining high-level and low-level data. A convolution block has been added to the output in order to create a map with no batch normalisation on both the encoder and decoder. Similar weights on both heads enhance GAN loss evaluation, but these changes produce a 2-headed Dr in which the decoding head trains the network. This implementation makes use of the real BigGAN PyTorch model.

3.3.8. U-Net Regularization

Although it is not always guaranteed, highly skilled Dr (Dr) strives to guarantee that the outcomes for every pixel in class-domain image alterations are comparable. To highlight the structural and semantic distinctions between phoney and authentic samples, consistency regularisation is used. To create synthetic graphics, CutMix augmentation entails cutting and pasting portions of many image classes. The most recent training sample for a Dr is produced as by combining the original image $r \in \times \times$ with the N masks, as determined by equations (6.7) and (6.8).

For a \mathbf{Dr}^U , the newest training sample is created as $\tilde{\mathbf{a}}$ through the combination of the original image $\mathbf{Gr}(\mathbf{c}) \in \mathbf{R}^{V \times I \times C}$ with the \mathbf{N} masks is assessed in equations (6.7) and (6.8).

$$\begin{aligned}\tilde{\mathbf{a}} &= \text{mixi}(\mathbf{a}, \mathbf{Gr}(\mathbf{c}), \mathbf{N}) \\ \text{mixi}(\mathbf{a}, \mathbf{Gr}(\mathbf{c}), \mathbf{N}) &= \mathbf{N} * \mathbf{a} + (\mathbf{1} - \mathbf{N}) * \mathbf{Gr}(\mathbf{c})\end{aligned}\quad (7)$$

$\mathbf{R}^{V \times I \times C}$ represents the image resolution, where \mathbf{V} is the height and \mathbf{I} is the width of an image. A binary mask $\mathbf{N} \in \{0, 1\}^{V \times I}$ indicates whether a pixel (j, i) appears in true ($N_{j,i} = 1$) or false ($N_{j,i} = 0$) image. $(*)$ is represented as an element-wise growth technique. For the new $\tilde{\mathbf{a}}$ CutMix image, $(l = 0)$ is unwavering as fake. $\text{Dr}_{\text{encoder}}^U$ accurately detects the authenticity of a composite synthetic image. If not, the Gr initiates CutMix expansion on the produced samples, leading to uninvited artifacts. To ensure consistent per-pixel prediction $\text{Dr}_{\text{decoder}}^U(\text{mixi}(\mathbf{a}, \mathbf{Gr}(\mathbf{c}), \mathbf{N})) \approx \text{mixi}(\text{Dr}_{\text{decoder}}^l(\mathbf{a}), \text{Dr}_{\text{decoder}}^l(\mathbf{Gr}(\mathbf{c})), \mathbf{N})$ a regularization loss term is included in the Dr objective function, which is then used to train the Dr .

$$O_{\text{Dr}_{\text{decoder}}^{\text{dist}}}^{\text{consist}} = \|\text{Dr}_{\text{decoder}}^U(\text{mixi}(\mathbf{a}, \mathbf{Gr}(\mathbf{c}), \mathbf{N})) - \text{mixi}(\text{Dr}_{\text{decoder}}^U(\mathbf{a}), \text{Dr}_{\text{decoder}}^U(\mathbf{Gr}(\mathbf{c})), \mathbf{N})\|^2 \quad (8)$$

The O^2 norm is represented by the symbol $\|\cdot\|$. The loss term represented in equation (6.9) integrates the one-sided hyperparameter β , which is also included in the Dr goal described in equation (6.3). The expression for equation (6.10) is as follows:

$$O_{\text{Dr}^v} = O_{\text{Dr}_{\text{encoder}}^U} + O_{\text{Dr}_{\text{decoder}}''} + \beta O_{\text{Dr}_{\text{decoder}}'}^{\text{consist}} \quad (9)$$

The Gr objective, signified in equation (6.6), remains unaffected.

3.3.9. IMDE OPTIMIZATION MODEL

Multimodal Optimisation Problems (MMOP) are the focus of the Niching Competition-based Memetic Direction Exploitation (NC-MDE) technique. It makes use of supporting archive (SA) approaches and incorporates local search operations. The Archive, Niching Competition (NC), the algorithm's local search tactics, and the control mechanism for Differential Evolution (DE) parameters will all be covered in detail in the upcoming subsections.

3.3.10. NC Strategy

To balance exploration and exploitation, neighbourhood-based niching approaches are incorporated into evolutionary algorithms for MMOP, which do not require parameters or require particular parameter values. By competitively investigating alternative optima and sharing information among adjacent persons, niching guarantees a varied search. Through dynamic neighbourhood exploration, these methods increase variety and draw offspring to areas inside the search space. The original distribution of people determines how many optimal solutions there are. By promoting memetic evolution and streamlining search space exploration, it successfully finds several optima in the categorisation of DR.

The NC approach is used to implement the idea. Niche discovery, usually with speciation cluster niching, is the first step in every generation. By choosing the best person as the starting point and adding surrounding people until a predetermined number (often 5) is reached, the

population is divided into niches. After that, the surrounding individuals are removed. Search activity and subspace diversity, which represent the average fitness and adaptability of niche individuals, determine their potential after they have been identified.

This is computed using the following equation (6.11). The symbols "*see*" and "*,*" respectively, represent the seed fitness and niche average fitness. Niching-based MMOP separates specialized seeds j^{th} and i^{th} by $Dis_{j,i}$. The maximum distance between niches is $Dis_{maximum}$. The average fitness of niche f^{th} and t^{th} is denoted as $fit_{j,a}$ and $fit_{i,a}$. The minimum and maximum average fitness across all niches is $fit_a^{minimum}$ and $fit_a^{maximum}$.

3.3.11. SA Strategy

Potential solutions are stored using archive technology, which also helps to preserve demographic diversity in niche-based MMOP approaches over time. By consuming and contributing to the archives at the speciality level, the method allows users to actively participate in the mutation process. They facilitate the exploration of the multimodal space by serving as a support populace for the changing population. Individuals in the early stages of evolution usually make up the archival population. With the exception of the initial fitness assessment of archive persons, this approach helps preserve variation and save promising solutions without resulting in further function assessment expenses. Algorithm 6.1 provides the IMDE model's pseudocode.

Algorithm 6.1: Contract-Expansive U-Net Model
<div>1. Initialize population P and archive A.</div> <div>2. Set initial values for DE parameters.</div> <div>3. Combine P and A to form joint population PA.</div> <div>4. Apply niching method to segment PA into niches and compute potential values (Eq. 6).</div> <div>5. Perform NC (Niche Creation) process to generate niches and archive strategy.</div> <div>6. For each generation (j):</div> <div>7. For each individual P in archive A:</div> <div>8. Generate a random value $R \in [0, 1]$.</div> <div>9. Compute probability PR_j based on niche j.</div> <div>10. If $R < PR_j$:</div> <div>11. Apply DE/R/1 mutation scheme using individuals in niche j to generate mutation vector.</div> <div>12. Perform binomial crossover to create new individual \hat{in}.</div> <div>13. In niche j, replace the most similar individual with \hat{in} if \hat{in} has better fitness.</div>

14. Else:

15. Select a niche randomly using roulette wheel selection based on affinity values.

16. Randomly select individuals from chosen niche (without replacement).

17. Apply DE/R/1 mutation scheme to generate mutation vector.

18. Perform binomial crossover to create new individual `in`.

19. Compute fitness of new individual `in`.

20. End if.

21. End for.

22. Perform Adaptive Cauchy-based local search with probability SV to improve seed solution.

23. Update DE parameters via adaptation scheme.

24. If the highest number of generations is reached, stop. Else, return to step 6.

25. Output the seed solutions for each niche.

The algorithm starts by creating a joint community PA and initialising population P and A for DE. After that, PA is divided into niches employing niche techniques and the NC procedure is used to support archive strategy and create niches. The most similar individuals within each niche are paired after individuals in A undergo crossover and mutation. It is swapped out if fitness is at its peak; if not, an other speciality is selected at random. The local search is adaptively Cauchy-based, with DE parameters being updated till convergence. Lastly, speciality seed solutions are produced.

3.4. Adaptive Local Search

The Adaptive Local Search method utilizes a Cauchy-based strategy to enhance evolutionary seed solutions. Prior to this, a Gaussian distribution-based search method is employed, where a trial solution S is sampled near the seed solution SSS using a Gaussian distribution with a low standard deviation. If the trial solution SSS is more effective than S, it replaces S. This Gaussian-based method is effective for improving solutions that are near the optimal state.

To address situations where the solution SSS may not be close to the ideal, an adaptive local search technique is introduced. This method changes the search direction and step-size adaptively based on the performance of SSS. If the optimal direction lies between SSS and SSS, and if SSS produces a better fitness value than SSS, then the adaptive local search technique is applied to refine SSS based on the relative fitness of S and S.

This will change the sampling center, because the update of the step size depends on a

parameter called μ . Solutions are real vectors in D-space. The seed solutions rank on fitness that influences the direction and magnitude of local search. This allows for a better convergence toward more optimum solutions by considering the properties of local search.

3.5. Parameter Adaptation Using Differential Evolution (DE)

The DE technique focuses on parameter adaptation by maintaining a historical memory of previous scaling factors and crossover rates, which are termed H and HCross. For each generation, once a solution S is ready to undergo recombination, a random index SSS is selected. The DE method computes the recombination values using the scaling and crossover parameters, then updates the parameters based on the fitness of the offspring solutions.

Once recombination occurs, the scaling and crossover parameters are updated if the offspring is fitter than its original solution. The H and HCross values get updated in successive generations with the help of the weighted mean and weighted Lehmer mean, respectively, for the parameters, thus adapting the evolutionary process dynamically.

This adaptive mechanism ensures the continuous improvement of the quality of solutions while adjusting evolutionary search parameters to better explore the solution space.

Optimizing U-Net GAN Model with IMDE

The optimization technique used here is Improved Multi-Dimensional Evolutionary (IMDE). The goal is to minimize the total network error, which is computed as the mean error on the whole dataset. It aims at reducing the latter by improving the parameters of the model.

For the model above, in its form the fitness function is used, such that a decrease in error will improve the fitness value. Thus, it ensures the process will help move the model toward optimal solutions when a network neuron makes as good an output as possible prediction. In IMDE technique fine tuning of the network weights occurs; with better results after each step in an optimization procedure, one obtains final optimization over time.

IMDE allows the model to learn and adapt to its parameters more effectively in the training of deep learning models such as U-Net GAN. This therefore leads to a highly accurate and efficient model that will perform tasks like image segmentation or data reconstruction effectively.

4. Model Performance Analysis Discussions

This method employs an IMDE-UNet-GAN to perform the task of detecting and classifying DR fundus images. Results and evidences of this proposed approach are demonstrated on IDRiD, Messidor-2, and a real-time dataset considered as a training as well as testing dataset. Experimentation in the proposed technique has been carried out on a computer containing an 11th Gen Intel Core i5-11500 processor while all the development was performed in MATLAB. All experimentation has been carried out using evaluation methodologies available in type.

4.1 Performance Comparison Analysis

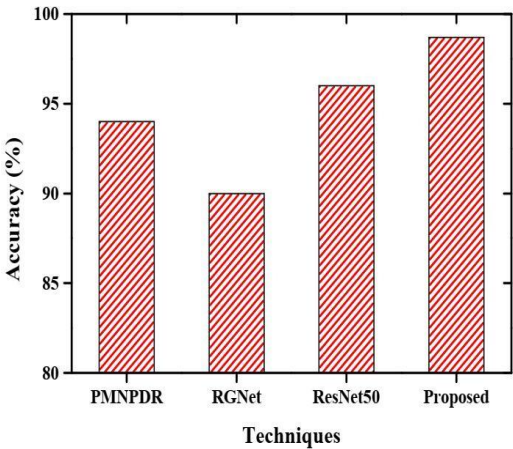
Figure 3(a) demonstrates the IMDE-UGAN model ACC, which is 98.89%, outperforming

existing models and proving superior results. In Figure 3(b), the IMDE-UGAN model achieves a recall of 98.48%, surpassing traditional techniques. Figure 3(c) shows the IMDE-UGAN model SEN at 98.54%, exceeding previous works. Finally, in Figure 3(d), the IMDE-UGAN model outperforms existing models with a SPE of 98.67%. These results highlight the effectiveness and efficiency of the IMDE-UGAN approach in detecting DR. Table 6.1 provides a comprehensive evaluation of the proposed model’s performance, comparing it to other existing models.

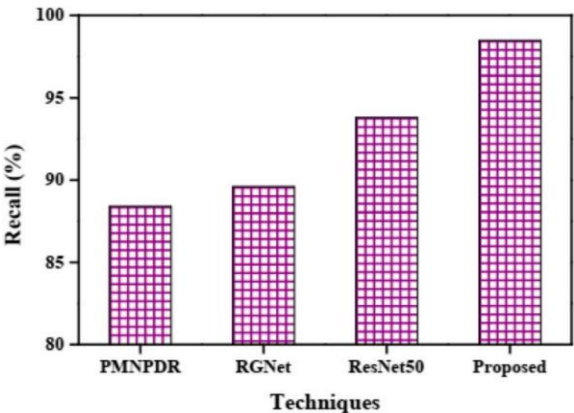
TABLE I. EXPERIMENTAL ANALYSIS OF IMDE-UGAN AND EXISTING MODELS

Models	ACC (%)	SEN (%)	SPE (%)	REC (%)
IMDE-UGAN (Proposed)	98.89	98.54	98.67	98.48
PMNPDR	94.5	90	96	88.4
RGNet	90	88	94	89.2
ResNet50	95.6	94	90	94.52

The IMDE-UGAN algorithm improves DR detection by optimizing parameters in the U-Net GAN model. It maintains diverse solution archives, minimizes segmentation errors, and integrates with SPADE ResNet-Encoder for accurate segmentation. TL enhances feature extraction, leading to improved DR stage detection in retinal images.



(a)



(b)

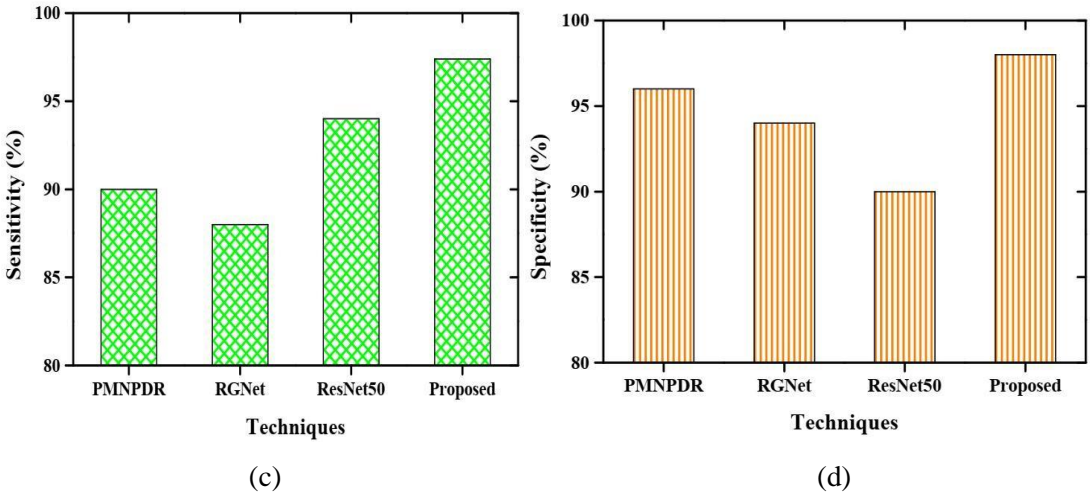


Figure 3. (a) Visual Comparison Results on ACC (b) Visual Comparison Results on Recall (c) Visual Comparison Results on SEN (d) Visual Comparison Results on SPE

Figure 4 illustrates the convergence graph comparing the IMDE-UGAN model with existing works. It shows the convergence of three optimization algorithms from existing works: Whale Optimization Algorithm (WOA), Particle Swarm Optimization (PSO), and Genetic Algorithm (GA), with the proposed IMDE algorithm.

The comparison indicates that the proposed algorithm outperforms the other three optimization algorithms. Table 2 presents a comparison of execution times between the IMDE-UGAN model and existing works. The existing algorithms GA, WOA, and PSO take 130, 102, and 97 seconds, respectively, to execute the trained dataset. In contrast, the proposed IMDE algorithm requires only 68 seconds for trained dataset execution.

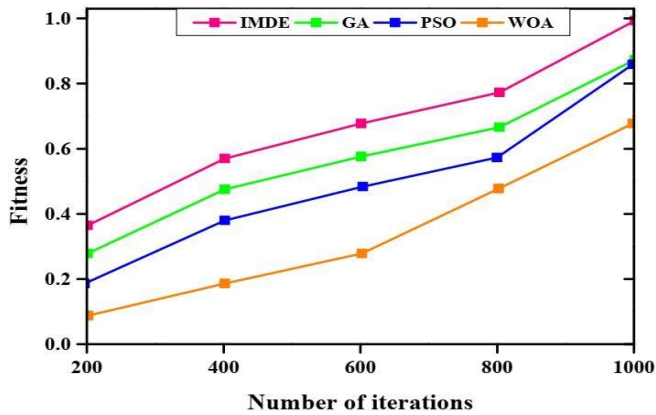


Figure 4. IMDE-UGAN and Existing Models Convergence Graph

TABLE II. COMPARISON OF EXECUTION TIMES

Optimization Algorithms	Execution Time of the Trained Dataset (Seconds)
GA Model	130s
PSO Model	102s
WOA Model	97s
IMDE (Proposed)	68s

Figure 5 compares ROC curves of the IMDE-UGAN model with three existing methods, evaluating their classification effectiveness across various thresholds using real-time and public datasets. PMNPDR, RGNet, and ResNet50 are chosen for comparison because of their strong performance in DR classification compared to other models, making them suitable benchmarks for evaluating the proposed model's performance using ROC curves. PMNPDR achieves a AUC score of 0.96, while RGNet and ResNet50 each achieve scores of 0.95. In contrast, the IMDE-UGAN method achieves a ROC value of 0.98, demonstrating superior performance. The ROC graph clearly shows that the IMDE-UGAN model performs better in terms of classification. Figure 6 displays the ROC curve for the DR dataset, demonstrating superior AUC in classifying both DR and non-DR classes. The IMDE-UGAN model achieves an AUC of approximately 98.97%.

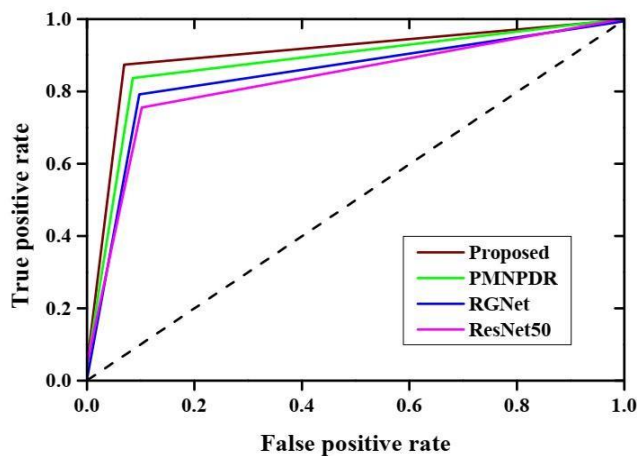


Figure 5. ROC Curve Comparison using Existing and IMDE-UGAN Model

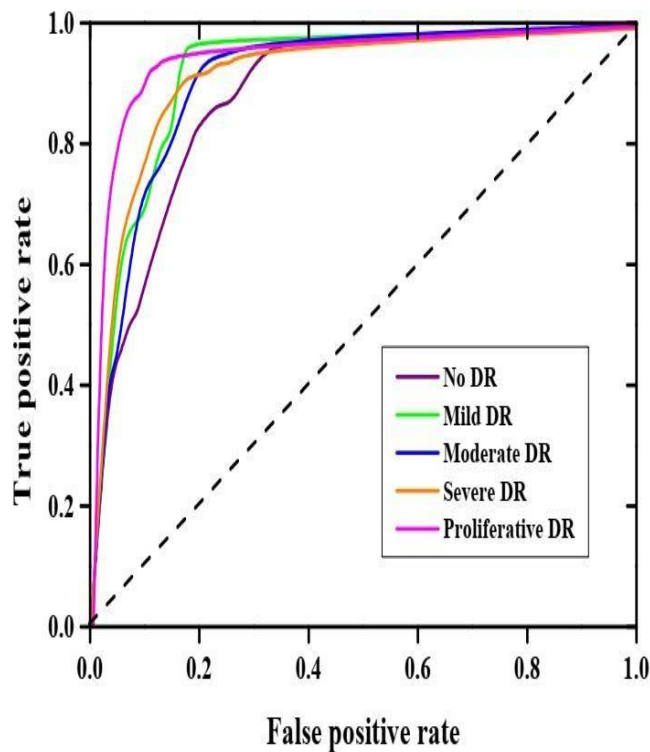

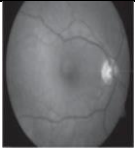
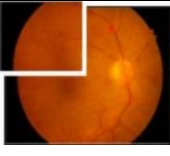

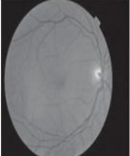
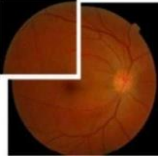


Figure 6. ROC Curve for DR Dataset

Table 6.3 presents the preprocessing and augmentation results for the IDRiD, Messidor-2, and ICF Hospital datasets. It demonstrates the transformation and augmentation process applied to the images for training and testing. Table 6.4 presents the classified images from the IDRiD, Messidor-2, and real-time datasets, along with their corresponding DR grades (grades 0-4). This table provides an overview of the classification results for each dataset, showing the distribution of different DR grades among the images.

TABLE III. IMAGE PREPROCESSING AND AUGMENTATION RESULTS USING IDRiD, MESSIDOR-2 AND REAL-TIME DATASETS

Dataset	Input image	Preprocessed	Augmented
IDRiD			
Messidor-2			

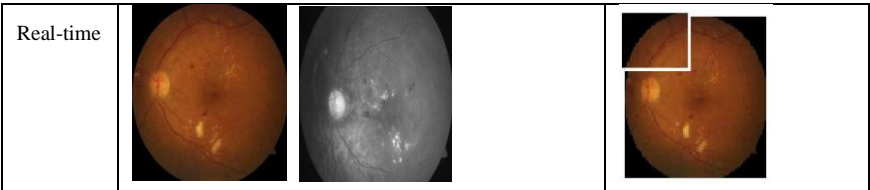
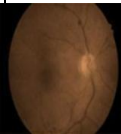


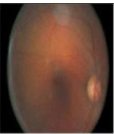
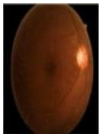


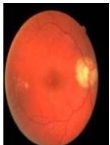
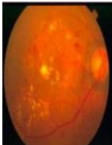




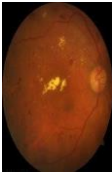
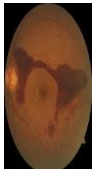


TABLE IV. SEVERITY GRADING RESULTS USING IDRiD, MESSIDOR-2 AND REAL-TIME DATASETS

Dataset	Grade-0	Grade-1	Grade-2	Grade-3	Grade-4
IDRiD					
Messidor-2					
Real-time					

Figures 7 (a and b) display the ACC and loss values for training and testing using the proposed model. This evaluates the testing ACC of both IMDE-UGAN and existing techniques, along with assessing ACC and loss values during training. The IMDE-UGAN model achieves the highest ACC as it trains on 80% of images and tests on 20%. Increasing the number of epochs decreases the duration of training and testing. With 100 epochs, the initial training loss of 0.30 decreases to 0.2, and the testing loss decreases from 0.20 to 0.12. These results indicate significant improvements in minimizing losses and increasing ACC with the proposed model.

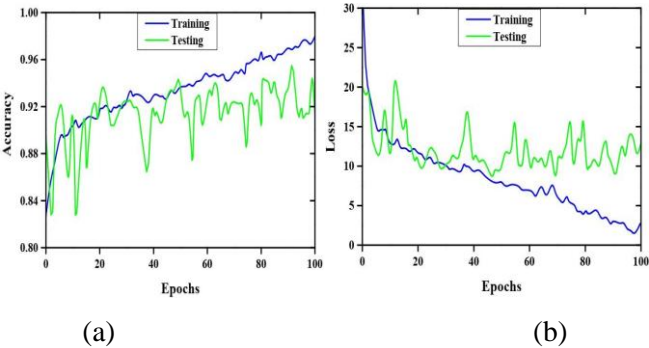


Figure 7. (a) and (b) ACC and Loss of Training and Testing using IMDE-UGAN Model

Figure 8 shows the accurately classified DR grading from the proposed model using the dataset collected from the hospital. Table 6.5 displays the hyper- parameter settings of the U-Net model.




Input			
Predicted Output	Grade 4	Grade 3	Grade 1
Actual Output	Grade 4	Grade 3	Grade 1

Figure 8. Accurate Categorized Results of IMDE-UGAN Model using Real-time Dataset

TABLE V. HYPER-PARAMETER OF U-NET MODEL

Hyper-parameters	Ranges
Batch size	16
Learning rate	0.001
Dropout	0.2
Optimizer	Adam
Epochs	20

Table 6.6 presents the ACC performance of the IMDE-UGAN and existing methodologies for Grades 0- 4 classes. The Grade0 performance for IMDE-UGAN model is 98.72%, Grade1 is 98.43%, Grade2 is 98.21%, Grade3 is 98.17%, and Grade4 is 98.64%. PMNPDR, RGNet, and ResNet50 exhibit lower performance compared to the IMDE-UGAN technique. Figure 9 (a and b) illustrates the ACC of IDRiD and Messidor-2 datasets with and without augmentation. It shows that both datasets have low ACC without augmentation but achieve good ACC with the augmentation process. Augmenting both datasets improve the performance significantly.

TABLE VI. INDIVIDUAL GRADING CLASS ACC ANALYSIS

Techniques	Grade0	Grade1	Grade2	Grade3	Grade4
IMDE-UGAN Model (Proposed)	98.72%	98.43%	98.21%	98.17%	98.64%
PMNPDR	85.12%	84.13%	85.18%	84.17%	84.57%
ResNet50	89.51%	88.59%	88.12%	88.13%	88.21%
RGNet	84.46%	83.42%	84.32%	82.41%	83.43%

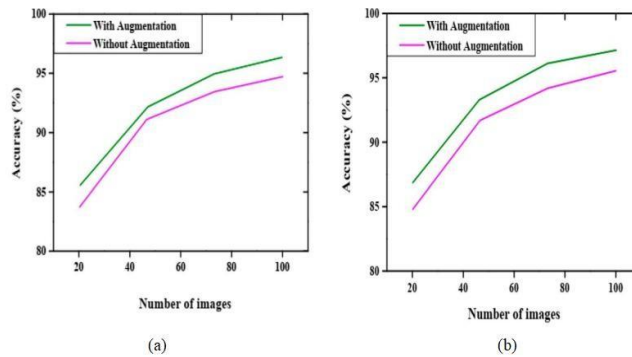


Figure 9. (a) and (b) Augmented vs Unaugmented ACC Comparison using IDRiD and Messidor-2 Dataset

4.2 ANALYTICAL STATISTICS

Due to ocular insults and hypoxia damage, imbalanced angiogenic and antiangiogenic factors can lead to the formation of neo vessels. Table 6.7 presents a statistical comparison between the IMDE-UGAN model and other existing techniques. The IMDE-UGAN approach was compared to existing methods using a t-test on the AUC model. A p-value below 0.05 rejected the null hypothesis. The best AUC achieved is 0.987, which surpasses that of previous approaches. The effect size is noted as es.

TABLE VII. COMPARISON OF STATISTICAL ANALYSIS

Models Used	AUC Value	t-test Value
IMDE-UGAN (Proposed)	98.7%	—
PMNPDR	91.2%	es = 1.111, P = 0.276
RGNet	87.6%	es = 7.432; P < 0.001
ResNet50	81.0%	es = 6.316; P < 0.001

4.3 PROBABILITY OF DR PREDICTION USING GRAPHICAL USER INTERFACE

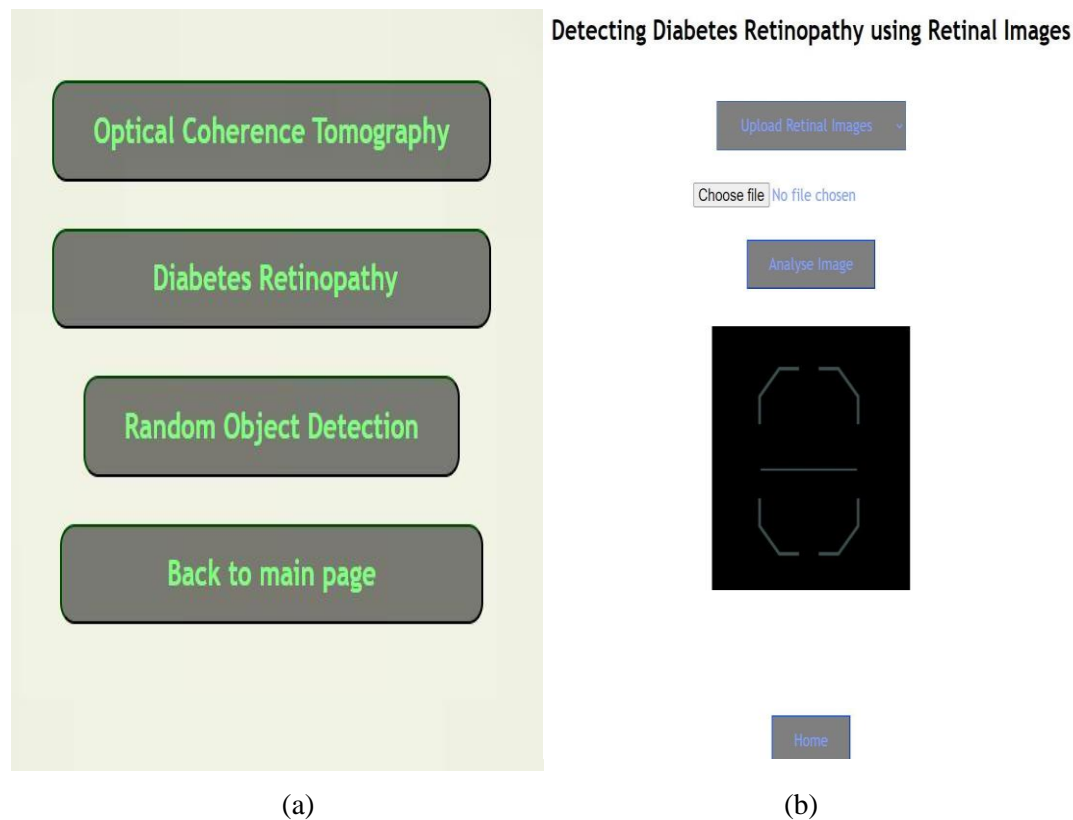
Development of a real-world DR prediction application using Python Flask framework for predicting 5-class probability using DR images.

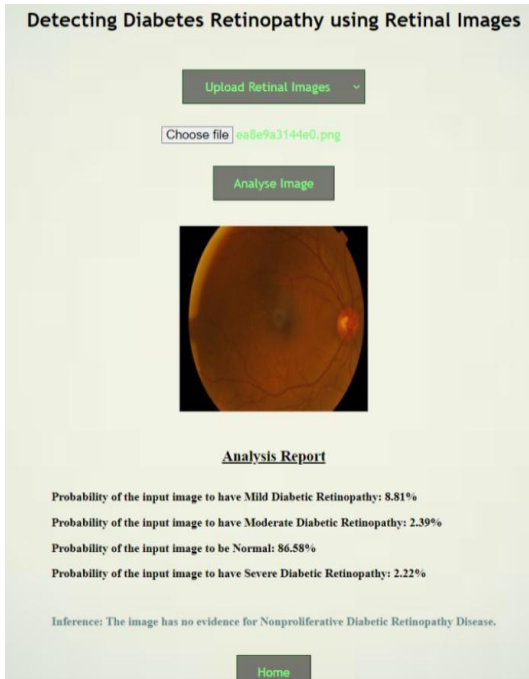
4.3.1 Application Development Process

- Utilize pre-trained models such as VGG16 to make predictions on test data, providing insights or classifications based on learned patterns and features.
- Leverage the Python Flask framework to create a user-friendly web application with features for routing, request handling, and templating, enabling rapid development.
- Deploy the web application on a local host for quick testing and debugging without external servers.
- Incorporate VGG16 into the application to allow users to upload images and receive predictions on the top 5 class probabilities directly in the browser interface.

The generated graphical user interface is improved by presenting the outcomes as the probability of predicting DR. After the image is uploaded and processed using the pre-trained model, the anticipated outcome and its related severity analysis report are shown on the HTTP page hosted by the local server at results.html. This web application is designed to detect and categorize two types of retinal diseases: OCT images and NPDR. The models utilized in the application are trained on publicly available datasets sourced from Kaggle. In addition to disease detection, the application offers a feature called random object detection. This functionality employs a pre-trained VGG16 model trained on ImageNet data. When applied to an image, the DR feature returns the top 5 class probabilities, indicating the objects the model identifies within the image.

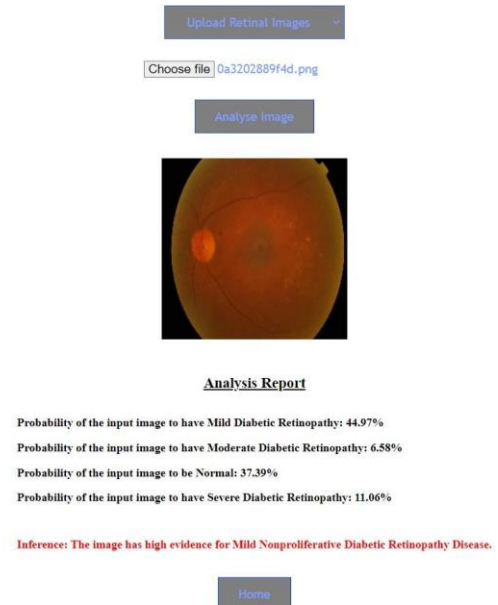
Figure 10(a) depicts the homepage of the user network, which is hosted on the local network accessible through the URL <http://192.168.202.220:80/home>. Figure 10(b) depicts the model pop-up page, which allows the user to upload a retinal fundus image to predict the presence of DR. Figure 10(c) displays the outcome of an uploaded fundus image indicating a high probability of no DR. Figure 10(d) illustrates the result of a fundus image with a high probability of Mild DR. Figure 10(e) exhibits the outcome of a fundus image with a high probability of Moderate DR. Lastly, Figure 10(f) demonstrates the result of a fundus image with a high probability of Severe DR.





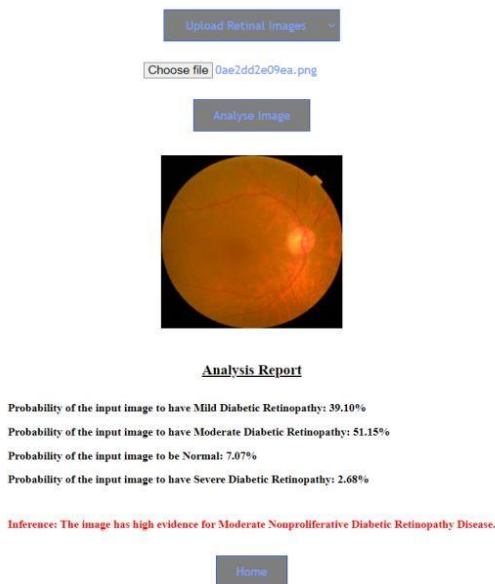
(c)

Detecting Diabetes Retinopathy using Retinal Images



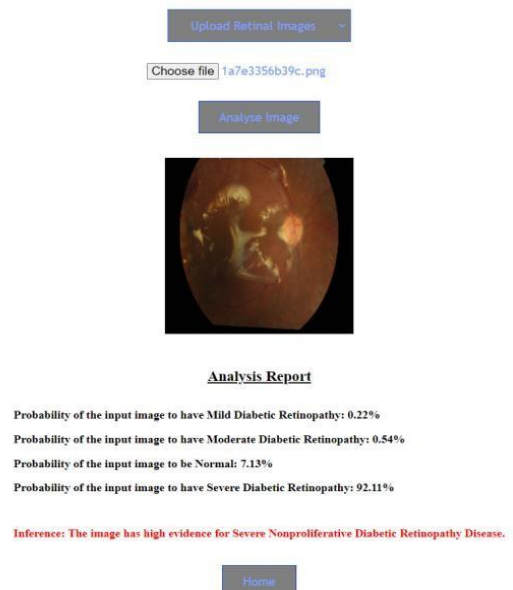
(d)

Detecting Diabetes Retinopathy using Retinal Images



(e)

Detecting Diabetes Retinopathy using Retinal Images



(f)

Figure 10. (a-f) Severity Grading of DR Prediction using Retinal Images

The Analysis report in the provided results indicates the probability of the retinal image being classified into the following stages: Normal, Mild, Moderate, or Severe DR. To enhance the front end, it is essential to include links that allow people to schedule consultations with experts specialized in DR. The research aims to enhance the detection of NPDR and PDR by finding additional blood vessels, which can serve as a preliminary test for PDR patients before consulting a doctor. Through this application, users can leverage advanced image analysis techniques to identify retinal diseases and severity prediction of DR with ACC. Additionally, the random object detection feature provides insights into the contents of images, enhancing the application's versatility and utility for users. The primary objective of the methodology is to assist clinical specialists in inefficiently and precisely diagnosing the Proliferative stage of DR disease. The ophthalmologists will be able to quickly measure diseases and abnormalities with the help of an automated tool that has been developed utilizing the VGG-16 net model.

5. Conclusion And Future Enhancements

This chapter proposes an optimization approach to classifying DR disease by grades. Each DR lesion has to be classified separately as it presents in a very different nature from others, and then results of all models combined in order to efficiently find out the grades of the disease. In this paper, an introduction has been given regarding DR classification by making use of IMDE- Contract-Expansive U-Net GAN model. It is one kind of algorithm to find multiple optima locations precisely. Optimization of parameters under the IMDE-Contract-Expansive U-Net GAN model, aiming to gain highly accurate DR detection and grading. With an optimized parameter, these ensure improved generalization along with better segmentations of images, more efficient representation of features to yield exact localization and accurate identification of the disease states. The DR image classification of Contract-Expansive U-Net GAN was used to implement by utilizing the modified architecture of U-Net for Dr. The given model was implemented and evaluated on datasets Messidor-2, IDRiD and the real-time dataset, with current models. According to the ACC, a higher value of 98.89% is reflected for the IMDE-Contract-Expansive U-Net GAN when compared to existing techniques whereas, for SEN, a 98.54% and, for SPE, it's a 98.67%. Significant improvements were observed in the ACC and loss across both models training and testing phases and lower loss and higher ACC. Improving the metrics on accuracy, precision, etc., in DR detection would be very crucial toward differentiating the several disease stages, from mild to very severe. Such stage differentiation is important so that treatments can be delivered early enough and appropriately. It would also be practical for mass screening in the resource-constrained setting by allowing rapid, reliable diagnoses on low-configuration computers and by reducing the critical shortage of ophthalmologists in developing countries through an initial diagnostic tool.

References

1. Choudhury, S., Bandyopadhyay, S., Latib, S., Kole, D., Giri, C.: Fuzzy c means based feature extraction and classification of diabetic retinopathy using support vector machines. In: 2016 International Conference on Communication and Signal Processing (ICCSP), IEEE, pp. 1520–1525 (2016)
2. Deng, H.: Interpreting tree ensembles with intrees. *Int. J. Data Sci. Anal.* 7(4), 277–287 (2019) Dutta,

- M. K., Srivastava, K., Ganguly, S., Ganguly, S., Parthasarathi, M., Burget, R., Prinosil, J.: Exudates detection in digital fundus image using edge based method & strategic thresholding. In: 2015 38th International Conference on Telecommunications and Signal Processing (TSP), IEEE, pp. 748–752 (2015)
3. Dutta, M.K., Parthasarathi, M., Ganguly, S., Ganguly, S., Srivastava, K.: An efficient image processing based technique for comprehensive detection and grading of nonproliferative diabetic retinopathy from fundus images. *Comput. Methods Biomech. Biomed. Eng.: Imaging Vis.* 5(3), 195–207 (2017)
 4. Gurudath, N., Celenk, M., Riley, H. B.: Machine learning identification of diabetic retinopathy from fundus images. In: 2014 IEEE Signal Processing in Medicine and Biology Symposium (SPMB), IEEE, pp. 1–7 (2014)
 5. Harini, R., Sheela, N.: Feature extraction and classification of retinal images for automated detection of diabetic retinopathy. In: 2016 Second International Conference on Cognitive Computing and Information Processing (CCIP), IEEE, pp. 1–4 (2016)
 6. Izenman, A. J.: Linear discriminant analysis. In: *Modern multivariate statistical techniques*, pp. 237–280. Springer, Amsterdam (2013)
 7. Kayal, D., Banerjee, S.: A new dynamic thresholding based technique for detection of hard exudates in digital retinal fundus image. In: 2014 International Conference on Signal Processing and Integrated Networks (SPIN), IEEE, pp. 141–144 (2014)
 8. Li, K., Qi, X., Luo, Y., Yao, Z., Zhou, X., Sun, M.: Accurate retinal vessel segmentation in color fundus images via fully attention-based networks. *IEEE J. Biomed. Health Inform.* 25(6), 2071–2081 (2020)
 9. Preethi, P., Saravanan, T., Mohanraj, R., & Gayathri, P. G. (2024). A real-time environmental air pollution predictor model using dense deep learning approach in IoT infrastructure.
 10. Palanisamy, P., Urooj, S., Arunachalam, R., & Lay-Ekuakille, A. (2023). A Novel Prognostic Model Using Chaotic CNN with Hybridized Spoofing for Enhancing Diagnostic Accuracy in Epileptic Seizure Prediction. *Diagnostics*, 13(21), 3382.
 11. Sandhya, N., Saraswathi, R. V., Preethi, P., Chowdary, K. A., Rishitha, M., & Vaishnavi, V. S. (2022, January). Smart attendance system using speech recognition. In 2022 4th International Conference on Smart Systems and Inventive Technology (ICSSIT) (pp. 144–149). IEEE.
 12. Asokan, R., & Preethi, P. (2021). Deep learning with conceptual view in meta data for content categorization. In *Deep Learning Applications and Intelligent Decision Making in Engineering* (pp. 176–191). IGI global.
 13. Majithia, S. et al. Cohort profile: The Singapore Epidemiology of Eye Diseases study (SEED). *Int. J. Epidemiol.* 50, 41–52 (2021). 54.
 14. Nguyen, H. V. et al. Cost-effectiveness of a National Telemedicine Diabetic Retinopathy Screening Program in Singapore. *Ophthalmology* 123, 2571–2580 (2016)..
 15. ElSayed, N. A. et al. 2. Classification and diagnosis of diabetes: Standards of Care in Diabetes—2023. *Diabetes Care* 46, S19–S40 (2023).
 16. Kaniadakis, G. et al. The κ -statistics approach to epidemiology. *Sci. Rep.* 10, 19949 (2020).
 17. He, K., Fan, H., Wu, Y., Xie, S. & Girshick, R. Momentum contrast for unsupervised visual representation learning. in *Proceedings of the IEEE/CVF conference on computer vision and pattern recognition* 9729–9738 (2020).
 18. Chen, X., Fan, H., Girshick, R. & He, K. Improved baselines with momentum contrastive learning. *arXiv preprint arXiv:2003.04297* (2020).
 19. Lundberg, S. M. et al. Explainable machine-learning predictions for the prevention of hypoxaemia during surgery. *Nat. Biomed. Eng.* 2, 749–760 (2018).
 20. Lundberg, S. M. & Lee, S. -I. A unified approach to interpreting model predictions. in *Advances in Neural Information Processing Systems* 30 (2017).